ISSN 8756-6990, Optoelectronics, Instrumentation and Data Processing, 2021, Vol. 57, No. 6, pp. 683–694. © Allerton Press, Inc., 2021.

COMPUTATIONAL AND DATA ACQUISITION SYSTEMS

Implementation of a Wavefront-Sensing Algorithm with Two-Channel Moiré Deflectometry and Matlab Graphic User Interface

Mohsen Dashti[1]* and Saifollah Rasouli[2,3]**

[1]*Department of Physics, Zanjan Branch, Islamic Azad University, Zanjan, Iran*
[2]*Department of Physics, Institute for Advanced Studies in Basic Sciences (IASBS), Zanjan, Iran*
[3]*Optics Research Center, Institute for Advanced Studies in Basic Sciences (IASBS), Zanjan, Iran*
Received October 29, 2021; revised December 17, 2021; accepted December 20, 2021

Abstract—Experimental setups of two-channel wavefront sensor (WFS) based on moiré deflectometry have been proposed and developed in recent years. Capabilities of this WFS have been tested in the atmospheric turbulence measurements. Like other WFSs, it can be used in various areas. Therefore, we have developed a MATLAB graphical user interface program to allow any user to easily use it. This program takes simultaneous horizontal and vertical moiré patterns as input data and reconstructs corresponding wavefront map and its aberration values. Algorithm of the process is explained step by step in this paper. For a typical input moiré pattern the results such as wavefront shape and corresponding first ten Zernike coefficients are calculated and are shown as outputs of the software. In addition, there is a special part in the program for the atmospheric turbulence applications that calculates strength amount of the turbulence, C_n^2, and temporal evolution of the angle of arrival.

DOI: 10.3103/S8756699021060169

Keywords: *wavefront sensor, MATLAB program, Moiré fringes, wavefront aberrations.*

1. INTRODUCTION

Wavefront sensors (WFSs) have many applications in optical metrology [1], adaptive optics [2], ophthalmology [3], etc. [4,5]. Measurements methods of WFSs are different. Some of them measure wavefront curvature such as curvature sensor [6] and some of them measure wavefront slopes such as Shack–Hartmann WFS [7]. Shack–Hartmann WFS is one of the most commonly used WFS that measures wavefront slopes. Shack–Hartmann WFS contains a lenslet array that focus an incident light beam on a detector such as a CCD. Distortions on the incident wavefront cause the movement of these spots. From the displacements of the spots on the CCD, phase slopes and the corresponding wavefront aberrations are calculated.

A new two-channel wavefront sensor based on moiré defelectometry (TChMD) was proposed by Rasouli et al. and developed in recent years [8]. It is used in the turbulence measurements [9, 10], but like other WFSs, it can be used in various applications. Experimental set-ups of this WFS are shown in Figs. 1 and 2. The set-up illustrated in Fig. 1a consists of two moiré deflectometers in two channels. There are two similar gratings in each channel that are separated by a Talbot distance. An appropriate coordinate system is chosen so that in the first channel the grating rulings are almost in the y-direction and those in the second channel are almost in the x-direction. When the first gratings are illuminated by an expanded and collimated laser beam, their self-images are formed on the second gratings, and, as a result, moiré fringes are formed in both of the channels. In the first channel, moiré fringes are in the x-direction and those in other channel are in the y-direction. Typical recorded moiré patterns using this

*E-mail: dashti.iauz@gmail.com,dashti_mohsen@znu.ac.ir
**E-mail: rasouli@iasbs.ac.ir

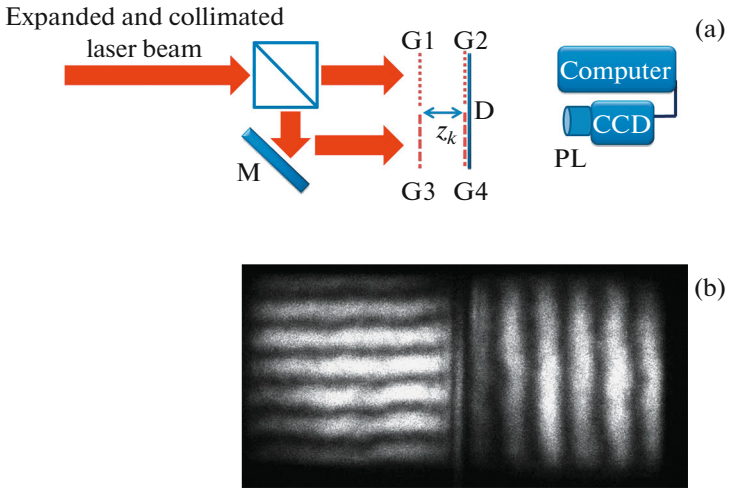

Fig. 1. (a) Schematic diagram of TChMD wavefront sensor set-up. BS, M, Z_k , D, and PL stand for beam splitter, mirror, Talbot distance, diffuser and projecting lens, respectively. G1, G2, G3, and G4 stands for gratings. (b) Typical recorded moiré patterns.

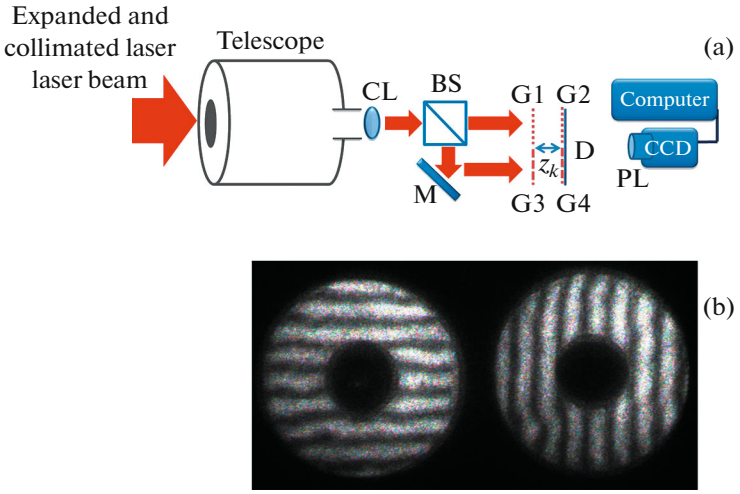

Fig. 2. (a) Schematic diagram of TChMD wavefront sensor set-up on a telescope. CL, BS, M, Z_k , D, and PL stand for collimating lens, beam splitter, mirror, Talbot distance, diffuser and projecting lens, respectively. G1, G2, G3, and G4 stands for gratings. (b) Typical recorded moiré patterns.

set-up are shown in Fig. 1b. The major limitation of this set-up is that reconstructed wavefronts are in the size of the gratings. To overcome this limitation, a telescope and a collimating lens could be added to the set-up (see Fig. 2a). In this case, magnification between first gratings and telescope entrance plane should be considered in calculations [10]. Typical recorded moiré patterns using this set-up are shown in Fig. 2b that, due to the telescope obscuration area, a dark zone is created in the center of moiré patterns.

As same as Shack-Hartmann WFS, distortions on the incident wavefront cause distortions on the moiré fringes. From deviations of the moiré patterns, one can determine phase slopes and corresponding aberration values. Moiré fringes are analyzed by a method that will be explained in detail in the next sections. We introduce a MATLAB graphical user interface (GUI) package that can helps anybody to use our WFS in a wide range of applications.

We consider six main parts in the program of the GUI as follows:

1. This program needs to take two sets of the moiré patterns; in the absence and present of the sample.

2. Removing high spatial frequencies from intensity distribution of the moiré patterns in order to get clear moiré patterns.

3. Finding the trace of the moiré fringes of the taken moiré patterns.

4. Finding the intersection points between horizontal and vertical traces for a given pair of moiré patterns.

5. Calculation of wavefront slopes and corresponding phase values from the displacements of the intersection points.

6. Decomposition of the wavefront into the primary Zernike modes.

In addition, we have considered a special part in the program for the atmospheric turbulence applications. One of the physical effects which is observed when a light beam propagates through a turbulent atmosphere is the fluctuations of light propagation direction. These fluctuations referred to as the fluctuations of the angle of arrival (AA). By calculation of the variance of AA fluctuations, one can determine strength amount of the optical turbulence, C_n^2. Using the procedure in reference [11], program calculates temporal evolution of AA and the value of C_n^2.

In continuance, we describe physical basis and corresponding equations of calculations in the program. After that, we will introduce different parts of our GUI package and show how a user can use it.

2. DATA ANALYSIS

In the TChMD wavefront sensor we need two sets of moiré patterns; moiré patterns in the absence and moiré patterns in the presence of the sample called reference and deviated moiré patterns, respectively. In some of applications, we deal with dynamic media such as atmospheric turbulence in which moiré fringes have randomly temporal evolution. In these cases, a long exposure time moiré patterns are recorded and used as reference moiré patterns. As it mentioned previously, due to the wavefront distortions moiré fringes deviate from their reference forms. In following, we describe how one can measure these deviations.

2.1. Getting Low Frequency Illumination

Since low spatial frequency in the recorded intensity distribution specified the moiré fringes, in order to get more clear moiré patterns, one can remove high spatial frequencies in the intensity distribution by use of Fourier transform method. In order that, Fourier transform of intensity distribution to be calculated and in the spatial frequency domain, high frequencies of spectrum are removed; then, inverse Fourier transform of the spectrum is calculated. In Fig. 3, moiré fringes before and after removing high spatial frequencies in the intensity distribution are shown and the corresponding intensity profiles along illustrated white line in the moiré pattern are presented.

2.2. Moiré Fringes Tracing

We call the locus of all of the points with maximum intensity along a given bright fringe as bright trace and the locus of all of the points with minimum intensity along a given dark fringe as dark trace. For determining the trace of given moiré fringe, one can use two different methods. In the first method a rectangular box has been chosen for a given moiré fringe so that only the desired fringe to be confined inside the box (see Fig. 4a). Intensity values in the box are saved as a matrix data. For a horizontal bright fringe, the locations of maximum for all of columns of the matrix, and for a vertical bright fringe, the locations of maximum for all of rows of the matrix are calculated. The locus of these maximum points is the trace of the fringe. For tracing of dark fringes, it is sufficient to calculate minimum intensities instead of maximum intensities in the tracing process. We named this method "box selecting method" in program. According to Fig. 4b, if we cannot choose a box in which to confined only a moiré fringe, the above method will not be appropriate to the moiré fringe tracing. In this case we need to use other algorithm to find the trace. In the second method we need select two points for each moiré fringe: one point at the beginning and another one at the end of a given fringe. Intensity value of the first point for a vertical fringe is compared with the pixel values on the right and left hand side of this point and for a horizontal fringe is compared with the pixel values on the top and below of this point. Then, maximum or minimum value of these three points is calculated and its coordinate is considered as the beginning of the trace. Then, we move down one pixel for a vertical fringe and move right one pixel for a horizontal

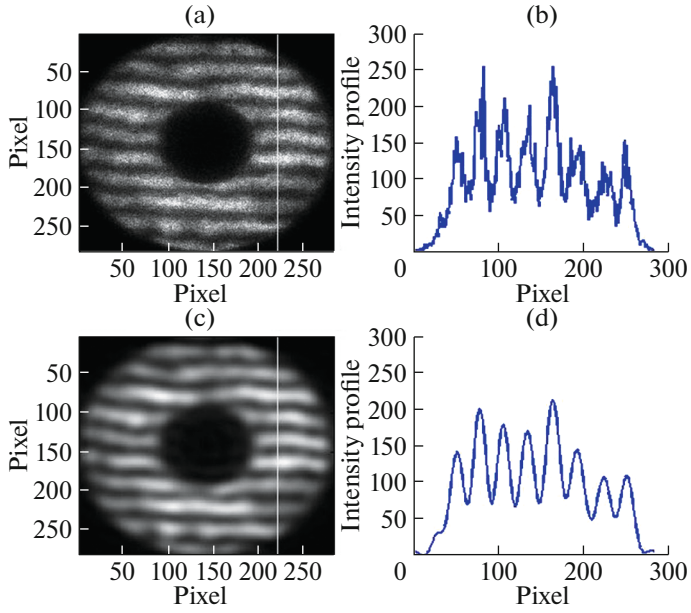

Fig. 3. (a) and (b) are typical moiré fringes in the study of atmospheric turbulence before and after removing high spatial frequencies in intensity distribution, respectively, (c) and (d) are the intensity profiles along illustrated white lines before and after high spatial frequencies removing, respectively.

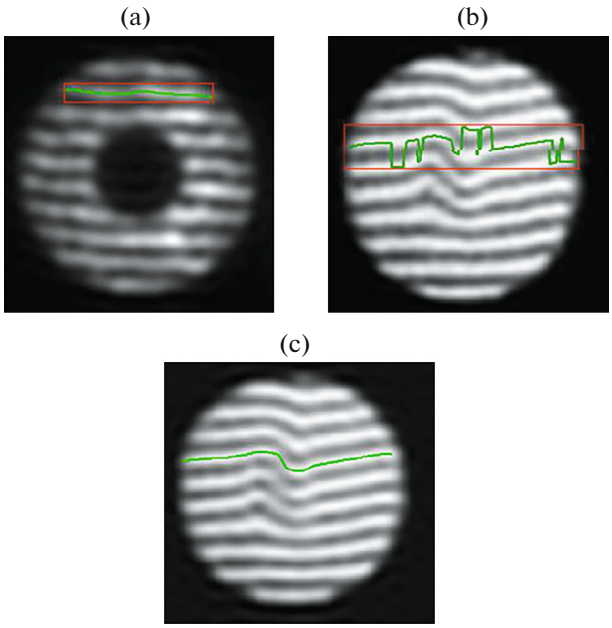

Fig. 4. (a) tracing of a moiré fringe using box selecting method, (b) incorrect tracing of a moiré fringe using box selecting method, (c) tracing of a moiré fringe using pixel by pixel method.

fringe and repeat the same procedure until we reach the end point of a fringe (see Fig. 4c). We named this method "pixel by pixel method" in program. In order to increase the spatial resolution of this work for a given moiré pattern 6 we introduce a new concept that we call virtual traces. As it mentioned previously one can remove high spatial frequencies using fast Fourier transform. After this work, the moiré fringes intensity profile in direction perpendicular to the moiré fringes can be written as

$$I(y) = \left[\left(\frac{I_\mathrm{b} + I_\mathrm{d}}{2}\right) + \left(\frac{I_\mathrm{b} - I_\mathrm{d}}{2}\right)\cos\frac{2\pi}{\mathrm{d_m}}(y + y_{0\mathrm{b}})\right], \tag{1}$$

where d_m, I_b, I_d, and $y_{0\mathrm{b}}$ are the moiré fringes spacing, the intensity of bright and dark traces, and the position of the reference bright trace, respectively. From Eq. (1), mid points between the adjacent bright and dark traces have an intensity equal to $I_\mathrm{vir}^{(1)} = \left(\frac{I_\mathrm{b} + I_\mathrm{d}}{2}\right)$. Now, for the case of distorted moiré pattern, the traces of points with intensities equal to the mean intensity of the adjacent bright and dark traces $I_\mathrm{vir}^{(1)} = \left(\frac{I'_\mathrm{b} + I'_\mathrm{d}}{2}\right)$ to be determined the first order virtual trace. By use of following equation in all of the columns of the intensity distribution of the moiré pattern, one can find the first order virtual trace

$$I_\mathrm{vir}^{(1)} = \left(\frac{I_\mathrm{b} + I_\mathrm{d}}{2}\right) = I'\left(y_\mathrm{vir}^{(1)}\right) \rightarrow y_\mathrm{vir}^{(1)} = y\left(\frac{I'_\mathrm{b} + I'_\mathrm{d}}{2}\right). \tag{2}$$

One can potentially produce a large number of virtual traces between two adjacent bright and dark traces by using their intensities and locations [12]. In order to specify all of traces in the same coordinate system, we should choose a coordinate system for all recorded moiré patterns.

2.3. Intersection Points

Similar to the array of the focal spots in the Shack–Hartmann WFS, an array of intersection points of the horizontal and the vertical traces are used in the TChMD WFS. In practice, these intersection points can be obtained by considering two sets of simultaneous vertical and horizontal moiré traces in one x-y coordinate system. This work should be done for both of reference and deviated moiré patterns. For calculation of the coordinates of the intersection points, we used a MATLAB code, intersections.m, written by Douglas M. Schwarz,[1] that we downloaded from the MATLAB web site. One can use functions such as polyxpoly that is defined in MATLAB toolbox, but the efficiency of the intersection.m is very high. In program, x and y-coordinates of all of the intersection points are set in $m \times n$ matrices individually that m and n are the total number of horizontal and vertical traces, respectively. We named these matrices for the reference traces by $XI0$ and $YI0$, and for the deviated traces by XI and YI. For example, XI_{ij} and YI_{ij} are the coordinates of intersection point between ith horizontal trace and jth vertical trace, but if in a case these traces do not intersect each other the corresponding elements of the matrices are set as NaN.

2.4. Displacement Vectors and Wavefront Slopes

We define the displacement of the moiré fringes matrices Dx and Dy in x direction and y-direction respectively, as follows

$$\begin{aligned} Dx &= XI - XI0, \\ Dy &= YI - YI0. \end{aligned} \tag{3}$$

Wavefront slope matrices can be written from the displacement matrices as follows

$$\left[\frac{\partial U}{\partial x}\frac{\partial U}{\partial y}\right]_{ij} = \frac{d}{z_k}\left[\frac{Dy}{d_\mathrm{mh}}\frac{Dx}{d_\mathrm{mv}}\right]_{ij}, \tag{4}$$

where U, d, d_mh, d_mv and z_k are the wavefront function, gratings period, horizontal moiré fringes spacing, vertical moiré fringes spacing and kth talbot distance, respectively. Different algorithms such as Fried geometry [13], Hudgin geometry [14], and Southwell geometry [15] are used to determine phase values from the wavefront slopes.

[1] http://www.mathworks.com/matlabcentral/fileexchange/11837

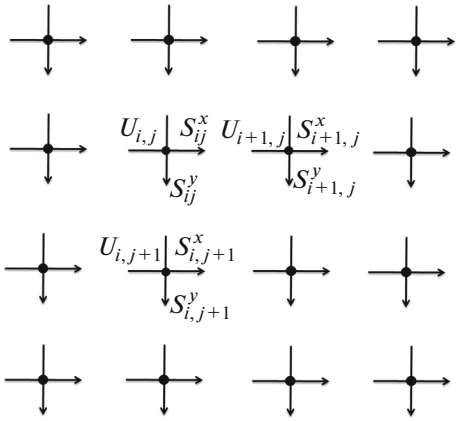

Fig. 5. Southwell geometry [15].

2.5. Wavefront Reconstruction

Since wavefront slopes are determined exactly on the intersection points and not between two adjacent intersection points, we have used Southwell geometry in program [15]. In this geometry, the relations between phase values and wavefront slopes are defined as follows

$$\frac{1}{2}\left(S^x_{ij} + S^x_{ij+1}\right) = \frac{U_{ij+1} - U_{ij}}{l}, \qquad (5)$$
$$\frac{1}{2}\left(S^y_{ij} + S^y_{i+1j}\right) = \frac{U_{i+1j} - U_{ij}}{l},$$

where $S^x_{ij} = \dfrac{\partial U_{ij}}{\partial x}$, $S^y_{ij} = \dfrac{\partial U_{ij}}{\partial y}$, and l is equal to the distance between two adjacent intersection points in the gratings plane. By considering these equations for all of the intersection points, a matrix equation, $\mathbf{S} = \mathbf{PU}$, is obtained, where $\mathbf{S}$ is a vector containing all of the slope measurements, $\mathbf{P}$ is named interaction matrix, and $\mathbf{U}$ is a vector of unknown wavefront values. By solving this equation, values of the wavefront function are obtained and phase values can be calculated from $\boldsymbol{\Phi} = \dfrac{2\pi}{\lambda}U$.

To determine aberration values, we expand phase function as sum of Zernike polynomials [16]

$$\boldsymbol{\Phi} = \sum_{i=1}^{\infty} a_i Z_i. \qquad (6)$$

We treat the above equation as a vector matrix multiplication [17]

$$\boldsymbol{\Phi} = \boldsymbol{Z}\boldsymbol{A}, \qquad (7)$$

where $\boldsymbol{\Phi}$ is the column matrix of the phase values and $\boldsymbol{Z}$ is a matrix in which each column is one of the Zernike polynomials, and $\boldsymbol{A}$ is the column vector of the Zernike coefficients. Program shows the wavefront map, corresponding Zernike polynomials map and their Zernike coefficients in the main window.

3. USING THE PROGRAM

By opening TChMD.m from MATLAB editor window and running it, the program could be started. The structure of the program, as a flowchart, is illustrated in Figure 6. Now, we introduce different parts in the main window of program in the next subsections.

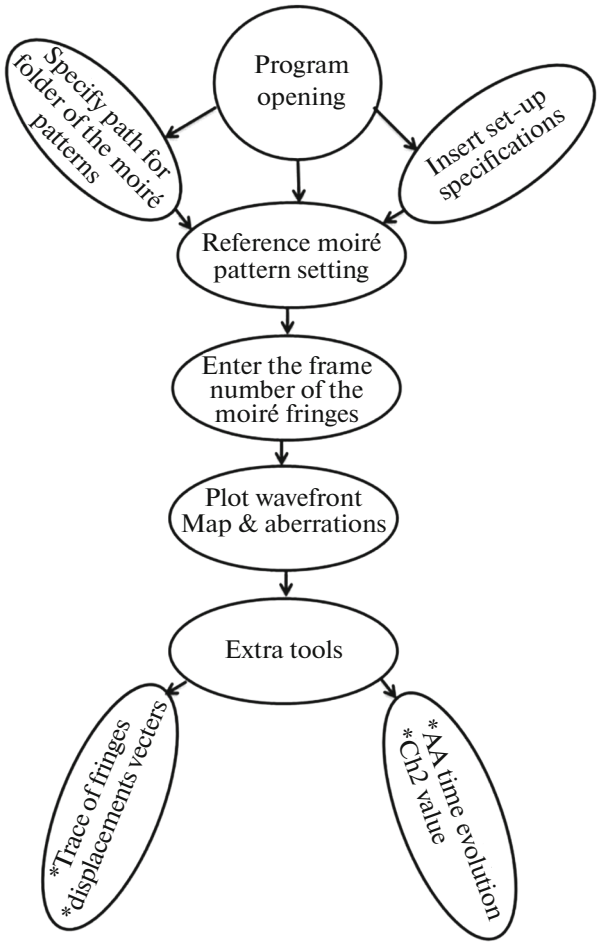

Fig. 6. Flowchart of the program structure.

3.1. Main Window

The main window of the program is shown in Figure 7. When a user runs the program, the main window that its name is TChMD will appear. Moiré fringes, wavefront map and aberrations map are shown in the different panels of the main window.

Moiré fringes—In this panel, the desired moiré patterns are represented. We assume that moiré patterns are recorded by a specific name that consist two parts; first part is a word and second part is a frame number. In the main window, user enters the frame number of desired moiré patterns to see corresponding wavefront map and its aberrations.

Wavefront map—By clicking on the plot button, the wavefront map of the selected moiré fringe will appear in this panel. User can switch between two-dimensional or three-dimensional plotting of the wavefront map.

Aberrations—By clicking the plot bottom, the program also calculates the value of the aberrations, and displays first 10 Zernike polynomials map except piston term in this panel.

3.2. Menus

3.2.1. File menu. When a user runs the program, the first thing that should be done is to specify the path where the folder of the moiré fringes is located. When user click on “Path Name of Images” from “File” menu, a small window will be opened in which user can specifies the address of recorded moiré fringes folder. In addition, user can save wavefront map and aberrations maps by clicking on Save option in “File” menu.

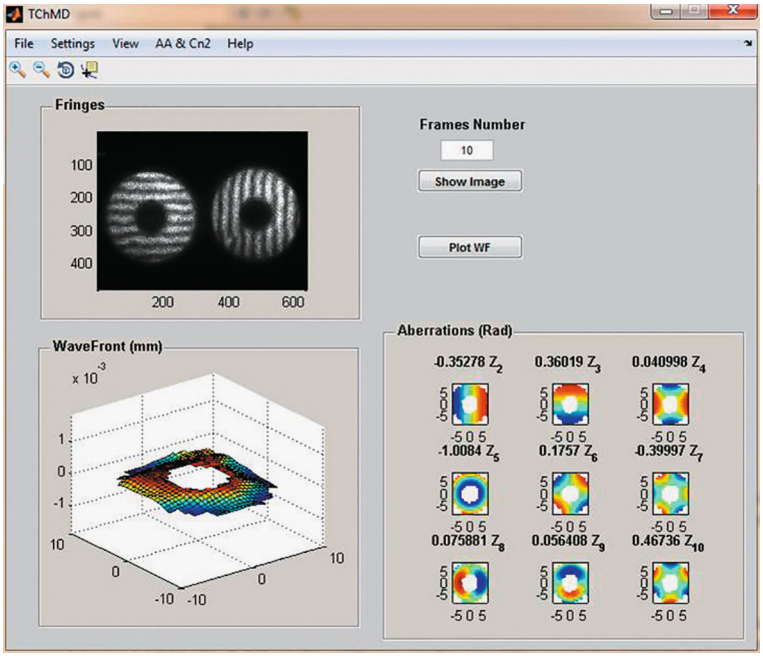

Fig. 7. Snap shot of the main window.

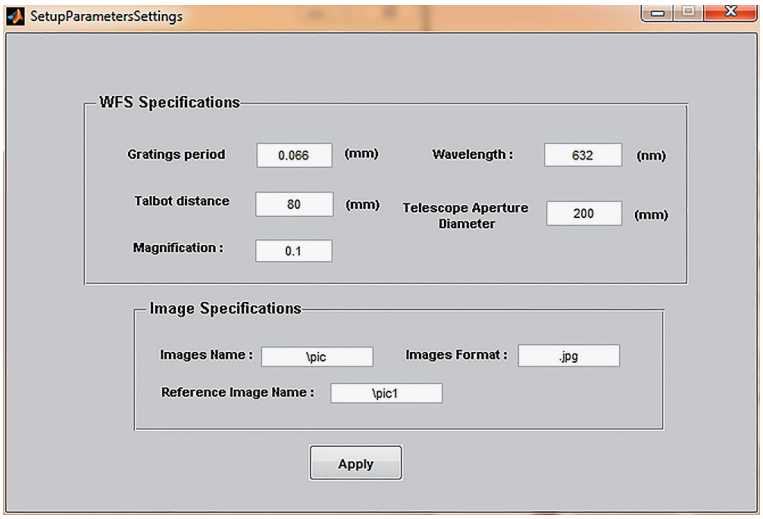

Fig. 8. Snap shot of the Set-up Parameters Settings sub-window.

3.2.2. Settings menu. In this menu two sub-windows are available. The first one is Set-up Parameters Settings sub-window. When user click "Set-up Parameters Settings" from the "Settings" menu, this sub-window will appear. User can enter WFS specifications such as gratings period, Talbot distance, telescope aperture diameter, magnification between the first gratings and telescope entrance plane and etc.

The second one is the Reference Frame Settings sub-window. In this sub-window, user can set the specifications of the reference moiré fringes such as horizontal and vertical moiré fringe spacing, dark area radius, bright area radius, and etc. As it mentioned in Section 2.1 for determining the trace of a fringe, high frequencies of intensity distribution could be eliminated. User sets the filtering radius as a cut-off spatial frequency in intensity distribution. Intensity profile in the direction perpendicular to the moiré fringe is plotted before and after elimination process and so user can identify the amount of the suitable radius. After clicking on the Apply button, Tracing sub-window will appear and user can determine the traces of the reference moiré fringes. There are two options for tracing method which the

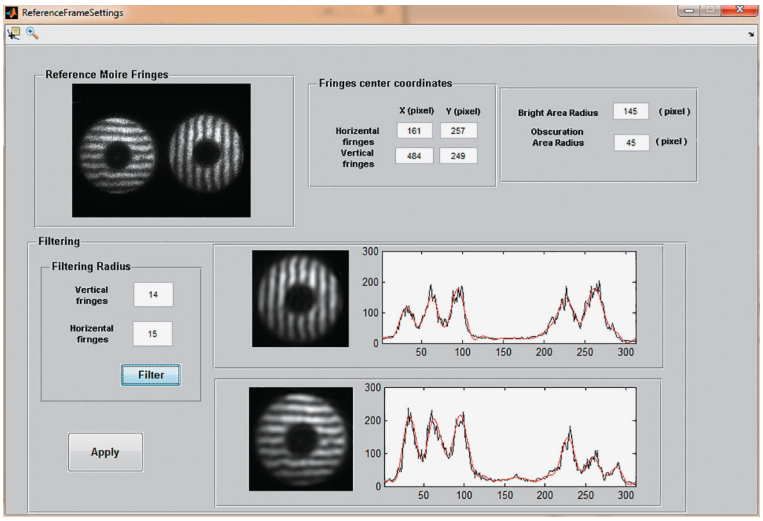

Fig. 9. Snap shot of the Reference Frame Settings sub-window.

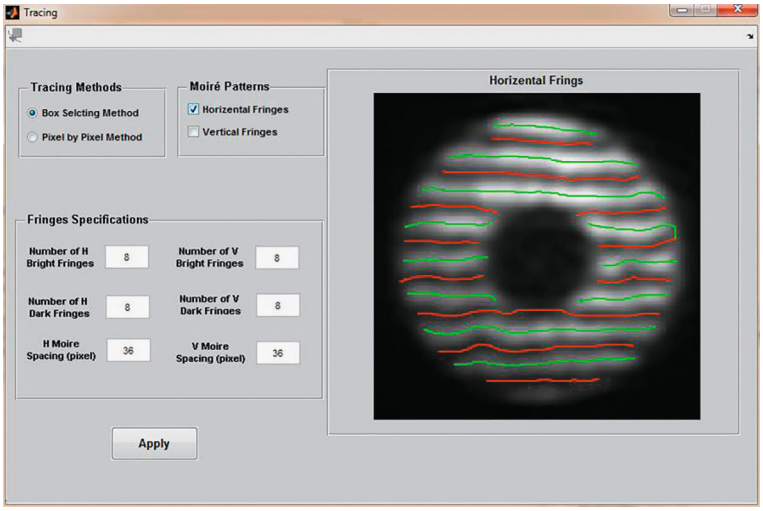

Fig. 10. Snap shot of the Tracing sub-window.

user can select one of them. After that by specifying the number of horizontal and vertical bright and dark moiré fringes the tracing process could be started. These sub-windows are shown in Figure 8 to Fig. 10.

3.2.3. View menu. In this menu user can see the Displacement Vectors sub-window (Fig. 11) and the Trace of Fringes sub-window (Fig. 12).

3.2.4. AA and C_n^2 menu. This part of the program is designed only for the turbulence study applications. When user clicks "AA & C_n^2" from the menu, user can see the angle of arrival evolution in successive moiré fringes. In addition, the user can enter the number of frames and the propagation distance to see the amount of turbulence strength, $C_n{}^2$. This sub-window is shown in Fig. 13.

3.2.5. Help menu. We provide a helping file in pdf format to make easily use of the software that is available in the help menu.

3.3. Program Features

– It is possible to change specifications of set-up in the program for different experimental set-up parameters.

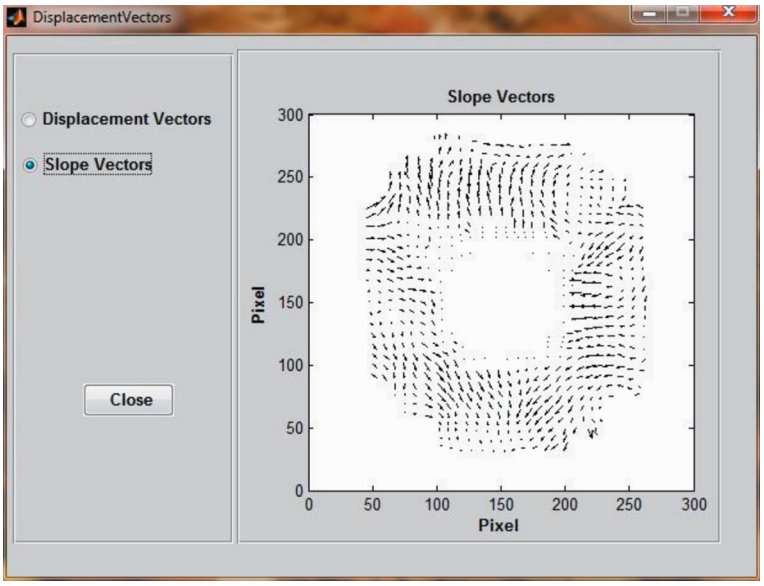

Fig. 11. Snap shot of the Displacement Vectors sub-window.

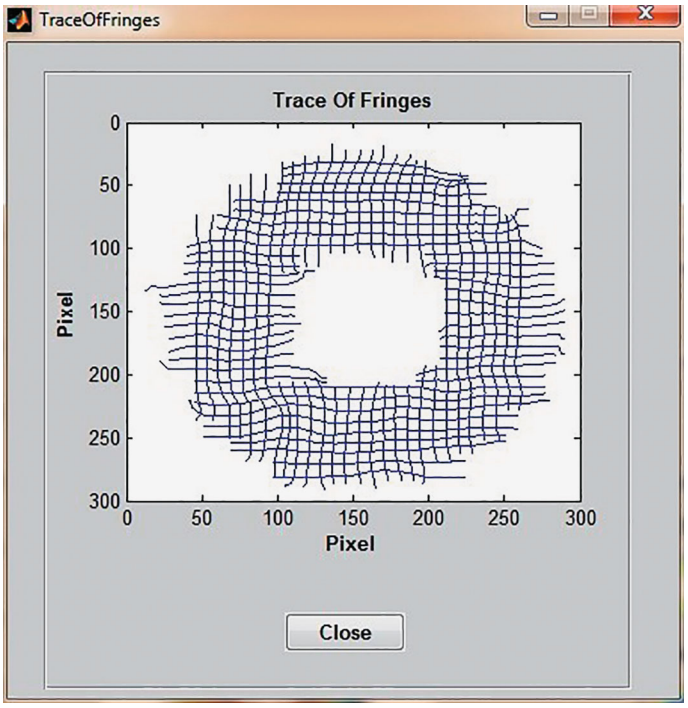

Fig. 12. Snap shot of the Trace of Fringes sub-window.

– Two different algorithms are used in program for tracing of moiré fringes which one is suitable for small deviation and another one for large deviation of the moiré fringes.

– Moiré fringes and corresponding wavefront and its aberrations are displayed simultaneously in the main window of the program, so the user can see intuitively how changes in moiré fringes cause the wavefront distortions.

– For turbulence applications, program has special part that calculate strength of turbulence C_n^2 and temporal evolution of the angle of arrival.

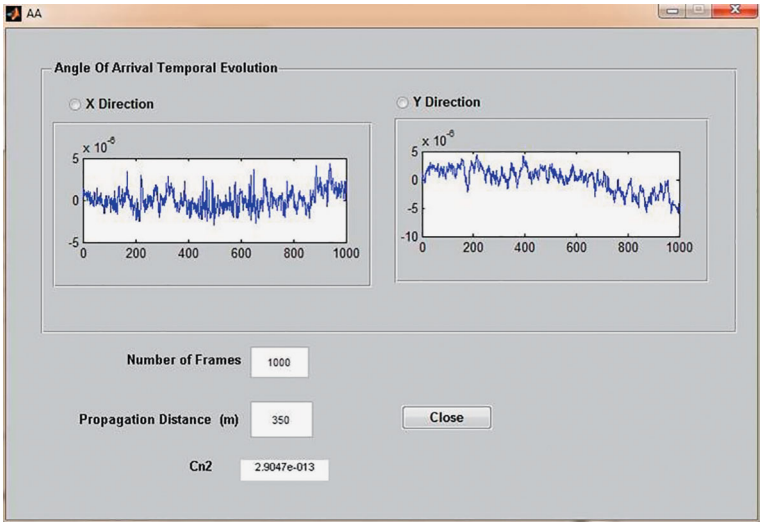

Fig. 13. Snap shot of the AA sub-window.

4. CONCLUSIONS

The developed program significantly increases the convenience of experimental measurement of wavefronts and the subsequent processing of the results of this measurement. Also This program is not only applicable for turbulence measurements [10, 18, 19] but also it can be used for any applications of a WFS [20, 21].

CONFLICT OF INTEREST

The authors declare that they have no conflicts of interest.

REFERENCES

1. C. Forest, C. R. Canizares, D. R. Neal, M. McGuirk, and M. L. Schattenburg, "Metrology of thin transparent optics using Shack–Hartmann wavefront sensing," Opt. Eng. **43**, 742–753 (2004). https://doi.org/10.1117/1.1645256
2. F. Roddier, *Adaptive Optics in Astronomy* (Cambrige Univ. Press, Cambridge, 1999)
3. N. Maeda, "Wavefront technology in ophthalmology," Curr. Opin. Ophthalmol. **12**, 294–299 (2001).
4. K. Murphy, D. Burke, N. Devaney, and C. Dainty, "Experimental detection of optical vorticeswith a Shack–Hartmann wavefront sensor," Opt. Express **18**, 15448–15460 (2010). https://doi.org/10.1364/OE.18.015448
5. D. Rativa, R. E. de Araujo, A. S. L. Gomes, and B. Vohnsen, "Hartmann-Shack wavefront sensingfor nonlinear materials characterization," Opt. Express **17**, 22047–22053 (2009). https://doi.org/10.1364/OE.17.022047
6. E. Roddier, "Curvature sensing and compensation: a new concept in adaptive optics," Appl. Opt. **27**, 1223–1225 (1988). https://doi.org/10.1364/AO.27.001223
7. B. C. Platt and R. Shack, "History and principles of Shack-Hartmann wavefront sensing," J. Refractive Surg **17**, S573–S577 (2001). https://doi.org/10.3928/1081-597X-20010901-13
8. S. Rasouli, A. N. Ramaprakash, H. K. Das, C. V. Rajarshi, Y. Rajabi, and M. Dashti, "Two channel wavefront sensor arrangement employing moiré deflectometry," Proc. SPIE **7476**, 74760K (2009). https://doi.org/10.1117/12.829962
9. S. Rasouli, M. Dashti, and A. N. Ramaprakash, "An adjustable, high sensitivity, wide dynamic range two channel wavefront sensor based on moiré deflectometry," Opt. Express **18**, 23906–23915 (2010). https://doi.org/10.1364/OE.18.023906
10. M. Dashti and S. Rasouli, "Measurement and statistical analysis of the wavefront distortions induced by atmospheric turbulence using two-channel moiré deflectometry," J. Opt. **14**, 095704 (2012). https://doi.org/10.1088/2040-8978/14/9/095704

11. S. Rasouli and M. T. Tavassoly, "Application of the moiré deflectometry on divergent laser beam to the measurement of the angle of arrival fluctuations and the refractive index structure constant in the turbulent atmosphere," Opt. Lett. **33**, 980–982 (2008). https://doi.org/10.1364/OL.33.000980
12. S. Rasouli, "Atmospheric turbulence characterization and wavefront sensing by means of the moiré deflectometry, in *Topics in Adaptive Optics*, Ed. by R. K. Tyson (IntechOpen, London, 2012). https://doi.org/10.5772/31129
13. D. L. Fried, "Least-square fitting a wave-front distortion estimate to an array of phase difference measurements," J. Opt. Soc. Am. **67**, 370–375 (1977). https://doi.org/10.1364/JOSA.67.000370
14. R. H. Hudgin, "Wave-front reconstruction for compensated imaging," J. Opt. Soc. Am. **67**, 375–378 (1977). https://doi.org/10.1364/JOSA.67.000375
15. W. H. Southwell, "Wave-front estimation from wave-front slope measurements," J. Opt. Soc. Am. **70**, 998–1006 (1980). https://doi.org/10.1364/JOSA.70.000998
16. R. J. Noll, "Zernike polynomials and atmospheric turbulence," J. Opt. Soc. Am. **66**, 207–211 (1976). https://doi.org/10.1364/JOSA.66.000207
17. J. D. Schmidt, *Numerical Simulation of Optical Wave Propagation with Examples in MATLAB* (Bellingham, Wash.: SPIE Press, 2010).
18. E. M. Razi and S. Rasouli, "Impacts of the source temperature and its distance on the statistical behavior of the convective air turbulence," Appl. Phys. B **125**, 185 (2019). https://doi.org/10.1007/s00340-019-7296-7
19. E. M. Razi, S. Rasouli, M. Dashti, and J. J. Niemela, "A high-resolution wavefront sensing method to investigate the annular Zernike polynomials behaviour in the indoor convective air turbulence in the presence of a 2D temperature gradient," J. Mod. Opt. **68**, 994–1001 (2021). https://doi.org/10.1080/09500340.2021.1968051
20. M. Yeganeh, S. Rasouli, M. Dashti, S. Slussarenko, E. Santamato, and E. Karimi, "Reconstructing the Poynting vector skew angle and wavefront of optical vortex beams via two-channel moiré deflectometry," Opt. Lett. **38**, 887–889 (2013). https://doi.org/10.1364/OL.38.000887
21. M. D. Daemi and S. Rasouli, "Investigating the dynamic behavior of thermal distortions of the wavefront in a high-power thin-disk laser using the moiré technique," Opt. Lett. **45**, 4567–4570 (2020). https://doi.org/10.1364/OL.396830

Translated by M. Dashti